

The predictability of sea-breeze generated thunderstorms*

R. A. PIELKE¹, A. SONG², P. J. MICHAELS³, W. A. LYONS⁴ and R. W. ARRITT⁵

¹ *Department of Atmospheric Science, Colorado State University, Fort Collins, Colorado 80523*

² *Universities Space Research Association, 4950 Corporate Drive, Suite 100, Huntsville, AL 35806*

³ *Department of Environmental Sciences, Clark Hall, University of Virginia, Charlottesville, VA 22903*

⁴ *R*SCAN Corporation, Minnesota Supercomputer Center, 1200 Washington Avenue South, Suite 2170, Minneapolis, MN 55415*

⁵ *Department of Physics and Astronomy, University of Kansas, Lawrence, KS 66045*

(Manuscript received January 16, 1990; accepted in final form May 17, 1990)

RESUMEN

Un análisis de satélite geostacionario y de radar ilustra claramente las regiones preferentes en donde ocurren las tormentas al sur de Florida. Un análisis sinóptico de los patrones asociados con el clima, sugiere que una troposfera baja y media más húmeda conduce a un porcentaje mayor de áreas cubiertas por estas tormentas.

Las configuraciones de convección profunda observadas pueden explicarse, en cierta medida, por regiones de aumento de convergencia horizontal de mesoescala en la capa límite, y la resultante acumulación de humedad en la troposfera baja.

Esta convergencia es incrementada al sur de Florida por la favorable curvatura del litoral (Pielke, 1984, p 458). Un modelo de mesoescala aporta una herramienta efectiva para simular las configuraciones observadas como función del viento sinóptico y la estructura termodinámica.

En general el flujo atmosférico de mesoescala tiene influencia en el ambiente sinóptico preexistente, de modo que suministra áreas preferentes de actividad de tormentas. Usando una combinación de radar, satélite, observaciones sinópticas y herramientas de modelos de mesoescala, predicciones efectivas del área cubierta y de la distribución espacial y temporal de tormentas en el ambiente de brisa marina parece ser posible en cualquier parte del mundo.

ABSTRACT

Geostationary satellite and radar analyses clearly illustrate preferential regions of thunderstorm occurrences over south Florida. A synoptic analysis of the associated weather patterns suggests that a moister lower and middle troposphere is conducive to a greater percentage of coverage by these storms. The observed patterning of deep convection can be explained to a large extent by regions of enhanced mesoscale horizontal boundary layer convergence and resultant accumulation of lower tropospheric moisture. This convergence is enhanced in south Florida by the favorable curvature of the coastline (Pielke, 1984, pg. 458). A mesoscale model provides an effective tool to simulate the observed patterns as a function of synoptic wind and thermodynamic structure.

In general, mesoscale atmospheric flow influences the preexisting synoptic environment so as to provide preferential areas of thunderstorm activity. Using a combination of radar, satellite, synoptic observations, and mesoscale modeling tools, effective predictions of the percent coverage, and spatial and temporal distribution of thunderstorms in the sea breeze environment anywhere in the world appears possible.

* This paper was originally prepared for the WMO International Workshop on Rain Producing Systems in the Tropics and the Extratropics, San José, Costa Rica, July 1986

1. Introduction

Sea breezes have been intensively observed (Hsu, 1969) and modeled (Pielke, 1974) for at least the last twenty years. A review of many of the investigations is presented in Pielke (1984, pgs. 456-464). As a result of these studies, a relatively clear understanding of the relation of the sea breeze to thunderstorm development and evolution has been achieved. This paper presents a brief summary of the relationship. Since south Florida has been extensively studied, the work reported in this paper will focus on that specific geographic location; however, the conclusions should be valid for any sea breeze environment.

2. Climatological studies

2.1 Synoptic data

Betts (1974), using composited tropical radiosonde soundings over Venezuela, showed that an increase in θ_e and decreases in θ_{es} and $(\theta_{es} - \theta_e)$ in the lower and middle troposphere were associated with increasing deep cumulus convective activity¹. Burpee (1979) found a similar result for south Florida.

McQueen and Pielke (1985) report on the variation of θ_e , θ_{es} , and $(\theta_{es} - \theta_e)$ over south Florida as a function of several surface geostrophic wind and direction classes. These data are related to satellite composite imagery as discussed in Section 2.2. Strong geostrophic flow was defined as greater than 3.5 m s^{-1} ; light and variable flow as less than 1 m s^{-1} . Figure 1 presents the

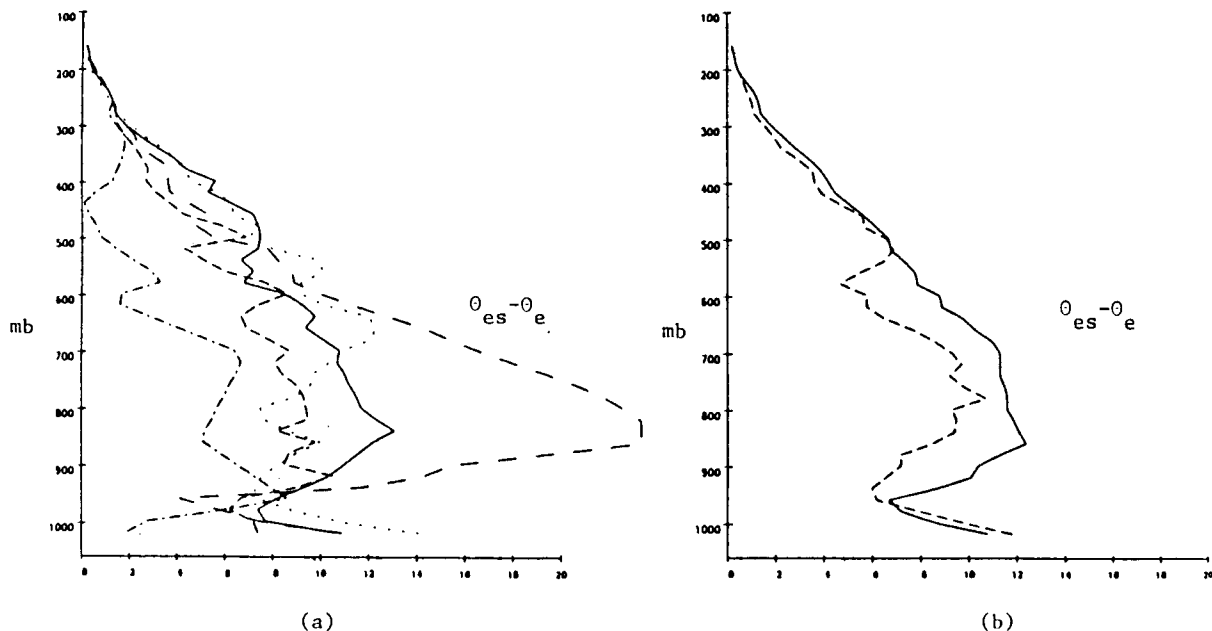


Fig. 1. Composite vertical profiles of the difference between saturated equivalent and equivalent potential temperature ($\theta_{es} - \theta_e$) in $^{\circ}\text{K}$ for (a) strong southeast (—), light southeast (---), strong east (· · · ·), very light and variable (— · — ·), and strong southwest (— · — ·) synoptic wind classes and (b) the averaged profiles for the undisturbed (—) and disturbed (---) synoptic classes. Vertical-ordinate axis is pressure in mb (from McQueen and Pielke, 1985).

¹ θ_e and θ_{es} are the equivalent and saturated equivalent potential temperature.

average profiles of $\theta_{es} - \theta_e$ for the several synoptic wind categories, and for undisturbed and disturbed² thunderstorm conditions as interpreted subjectively from the geostationary satellite imagery reported in the next section. While the sample size is small as shown in Table 1, so that the statistical significance is reduced, the disturbed days are somewhat moister than the undisturbed days, with the light and variable synoptic situations being particularly dry. Light and variable geostrophic flow in the latitude of south Florida during the summer is generally associated with a subtropical ridge center located directly over the region. The subsidence associated with this descending portion of the Hadley cell likely explains the drying and warming of the atmosphere, relative to the other flow situations. In addition, there is less moisture advection from the adjacent ocean when the synoptic winds are light.

	Synoptic Class (Number of Satellite Collect Days)	Percent Area of Deep Convection		$\overline{\theta_{es} - \theta_e}$ (°K)	
		\bar{x}	σ	\bar{x}	σ
1	Disturbed (6)	9.3	13.6	7.8	2.4
2	Strong Southeast (7)	7.9	5.1	10.0	2.3
3	All Undisturbed Days (28)	5.8	5.3	9.7	4.7
4	Strong East (7)	5.4	5.1	8.7	3.4
5	Light Southeast (6)	5.4	4.1	8.2	2.7
6	Light and Variable (4)	1.6	2.0	14.2	8.3

Table 1. The daily averaged percent and standard deviation of deep convection over the south Florida peninsula for each synoptic class. Synoptic classes are listed from most to least convectively active. The number in parentheses is the number of soundings available for that class (from McQueen and Pielke, 1985).

2.2 Satellite composites

During the summer of 1983, geostationary satellite imagery was analysed for 34 days at two hour intervals and composited using the same geostrophic wind and direction classes mentioned in Section 2.1. Regions of deep cumulus convection were identified as regions of bright clouds, determined quantitatively from the visible 0.8 km resolution images, and with cold tops, defined as less than -38°C , as evaluated from the infrared 13 km resolution imagery. While the limited sample size and substantial day-to-day variability limited the statistical significance of the results, interpretations from the data are felt to be instructive in explaining south Florida sea breeze deep convection. As reported in McQueen and Pielke (1985), the percentage of coverage of land and of water by deep cumulus convection was evaluated as a function of time of day (Figure 2). The diurnal variation in activity is clear in the figure although the case-to-case variance in percent coverage at a given time is quite high. The disturbed days apparently are somewhat less dependent on solar heating, though even here there is a noticeable peak in the early afternoon. Table 1 presents the average coverage during the day for the different synoptic categories with the dry and warm, light and variable case having the least percent of coverage. An example of

² Disturbed and undisturbed are defined subjectively based on satellite observation of extensive oceanic cloudiness adjacent to south Florida (see McQueen and Pielke, 1985, for details).

the composite diurnal variation in deep convection as viewed from the satellite is illustrated for light southeast geostrophic flow over south Florida in Figure 3.

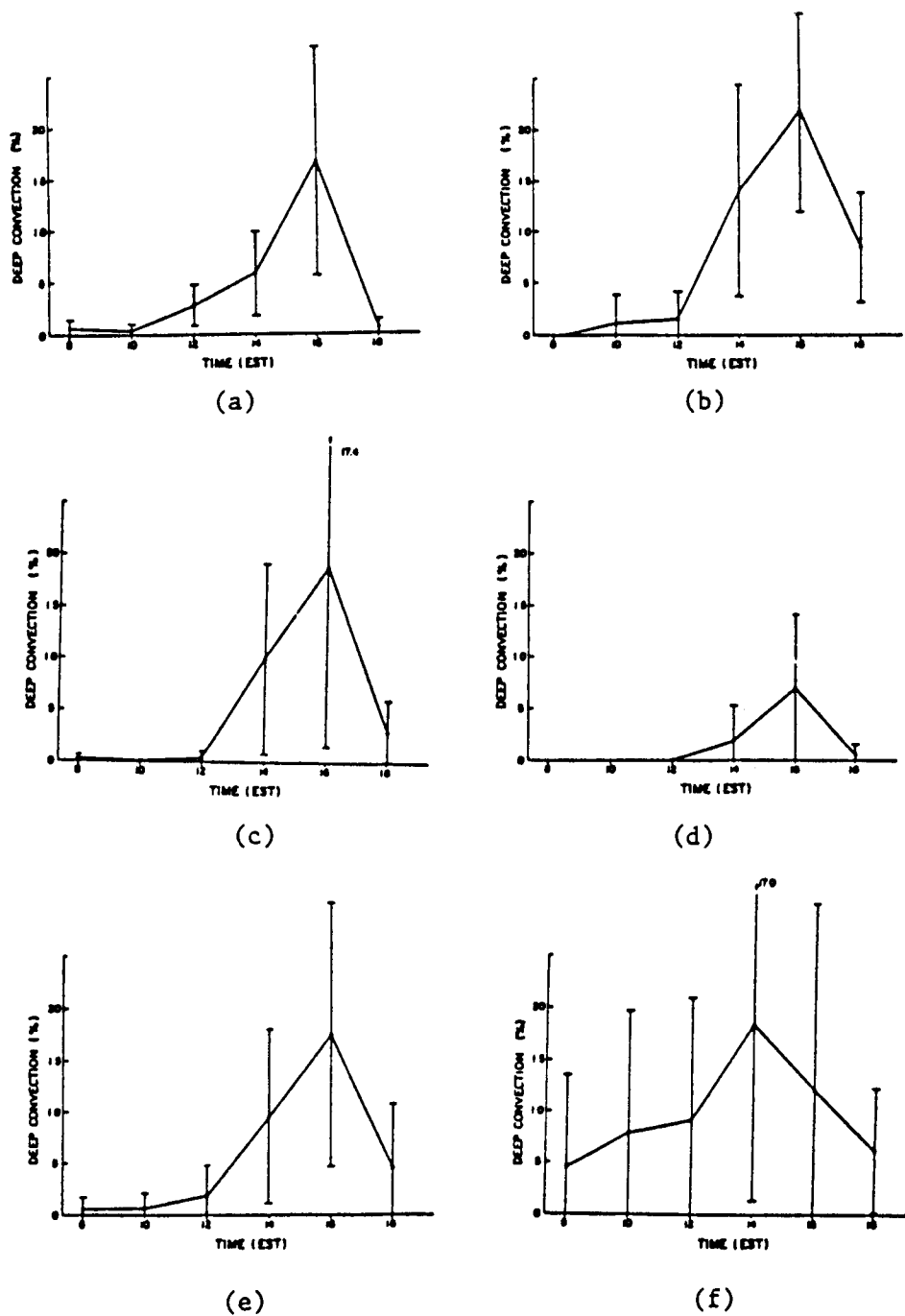


Fig. 2. Averaged percent of deep convective clouds for the various synoptic classes: (a) light southeast, (b) strong southeast, (c) strong east, (d) light and variable, (e) undisturbed, and (f) disturbed. The error bar corresponds to one standard deviation on either side of the mean (from McQueen and Pielke, 1985).

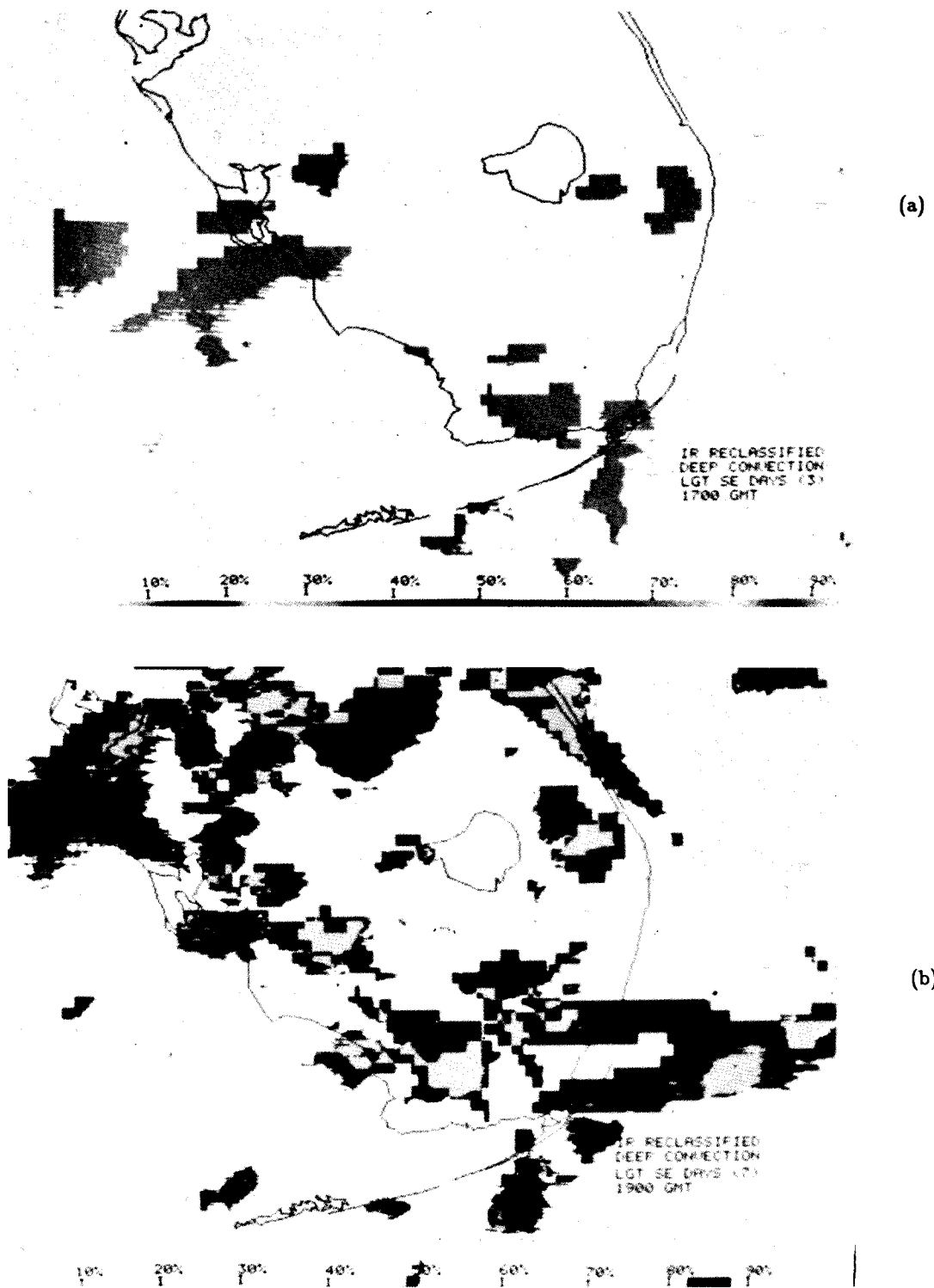


Fig. 3. Evolution of satellite-sensed convective patterns for light southeasterly flow: (a) 1200 EST; (b) 1400 EST; (c) 1600 EST; and (d) 1800 EST (from McQueen and Pielke, 1985).

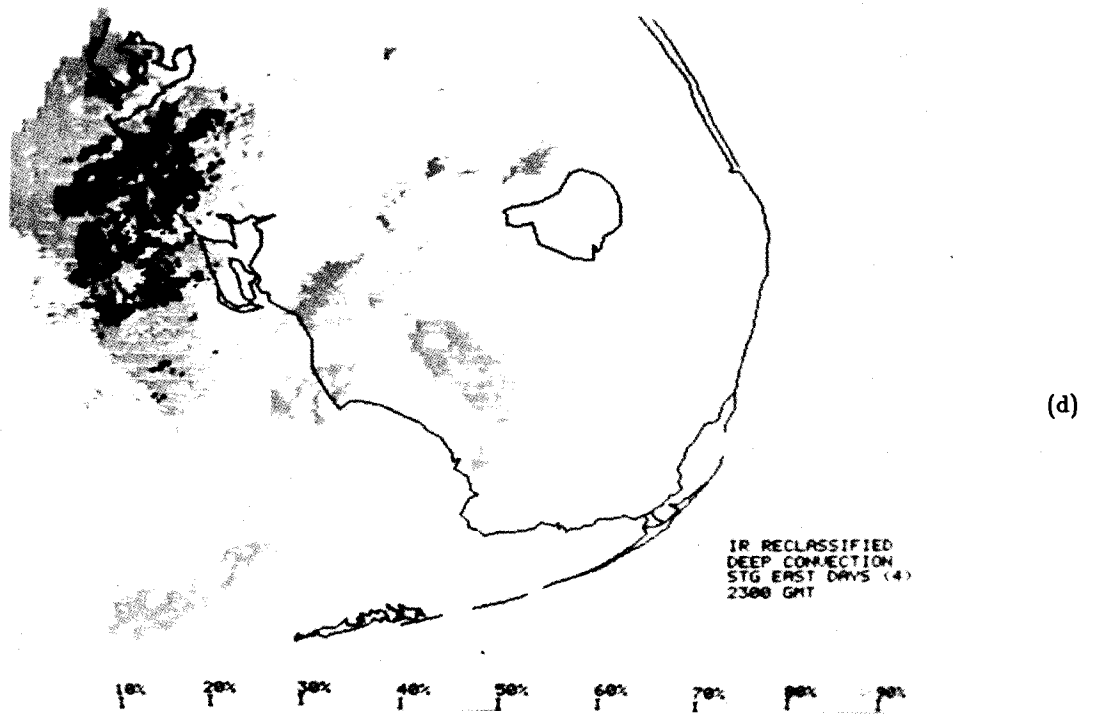
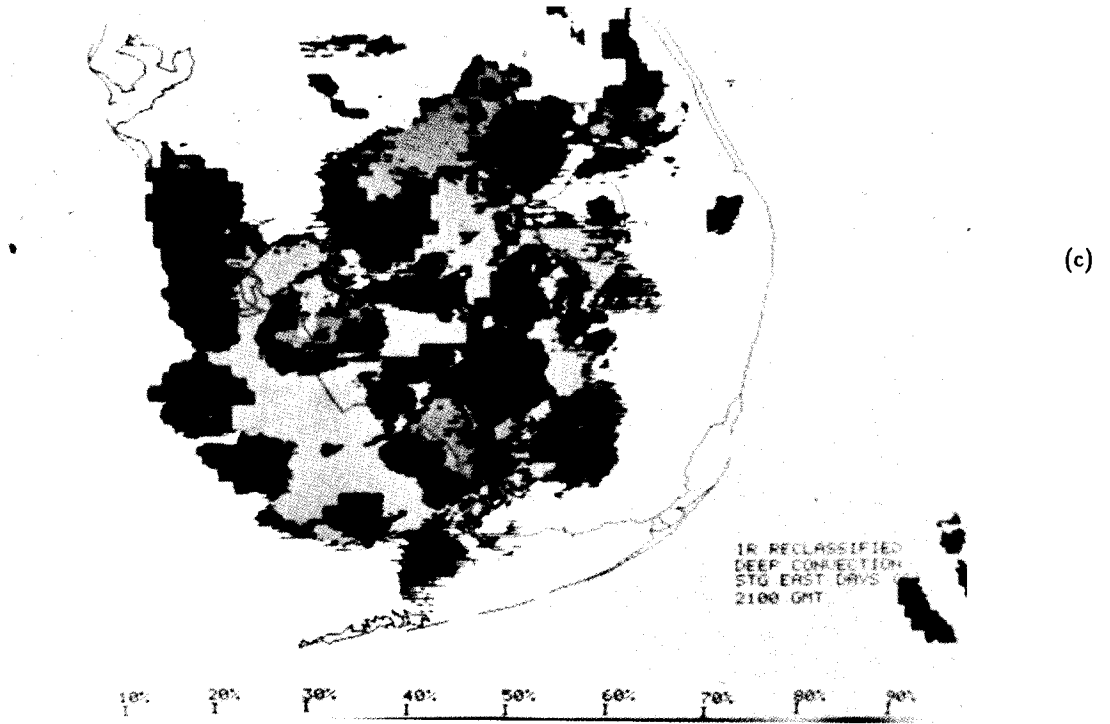


Figure 3 (continued)

Satellite observations of percentage of coverage of earlier deep convection can also be used to predict subsequent deep convection. Table 2 summarizes such an analysis over south Florida where deep convection over south Florida and over the adjacent ocean during the morning is related to the observed deep convection over the land at 1400 EST. Despite the small satellite composite sample size, the correlation is significant statistically between ocean deep convection at 0800 EST or land deep convection at 1000 EST, and the observed deep convection over land at 1400 EST. The reason for this correlation (which is stronger than the correlation between the radiosonde derived $\theta_{es} - \theta_e$ and deep convective activity) is likely that the observed deep cumulus activity is more representative of $\theta_{es} - \theta_e$ conditions over the region, than can be obtained from a single radiosonde ascent alone.

	Undisturbed		All Days		Light Wind		Strong Wind	
	R	Sig	R	Sig	R	Sig	R	Sig
% Deep Convection over Land at 0800 EST	.26	.23	.40*	.05	.61*	.04	.11	.78
% Deep Convection over Land at 1000 EST	.59*	.01	.44*	.03	.81*	.01	.55	.16
% Deep Convection over Water at 0800 EST	.44*	.05	.43*	.03	.74*	.01	.30	.43

Table 2. Correlation matrix between antecedent and subsequent deep cumulus convection at 1400 EST over land. Asterisks indicate significance values of 0.05 or better (from McQueen and Pielke, 1985).

2.3 Radar composites

In an attempt to extend the data base of preferred locations of deep cumulus convection over Florida from that available using geostationary satellite imagery, more than 10000 hours of high resolution ($47.6 \times 47.6 \text{ km}^2$) 24 hour manually digitized radar (MDR) data for June, July and August of 1978 to 1982 were analyzed for thunderstorms (defined as a video integrator and processor (VIP) reflectivity of three or greater, Reap and Foster, 1979). Further details are presented in Michaels *et al.* (1987). Figure 4 illustrates that the average hourly value of a reflectivity of three or greater is as high as 15% at two locations along the southwest Florida coast. Figure 5 documents that the percent of days during the study period in which at least one thunderstorm occurred somewhere in the analysis grid (an area of 2265 km^2) reached as high as 84% along the southwest coastal area. In the satellite composite analysis, maximum frequencies at a given time reached about 75% on the sampled days (Figure 3 at 1600 EST), in about the same locations. It is worth noting that the satellite had a smaller spatial sampling scale ($\sim 174 \text{ km}^2$) than the radar (2265 km^2).

The largest averages in Figure 4 are concentrated over smaller areas than the maximum daily average occurrence in Figure 5, apparently because there are more hours of activity during many days in these hourly average locations, but the likelihood of at least one thunderstorm during the day within a grid area is greater elsewhere in coastal southwest Florida.

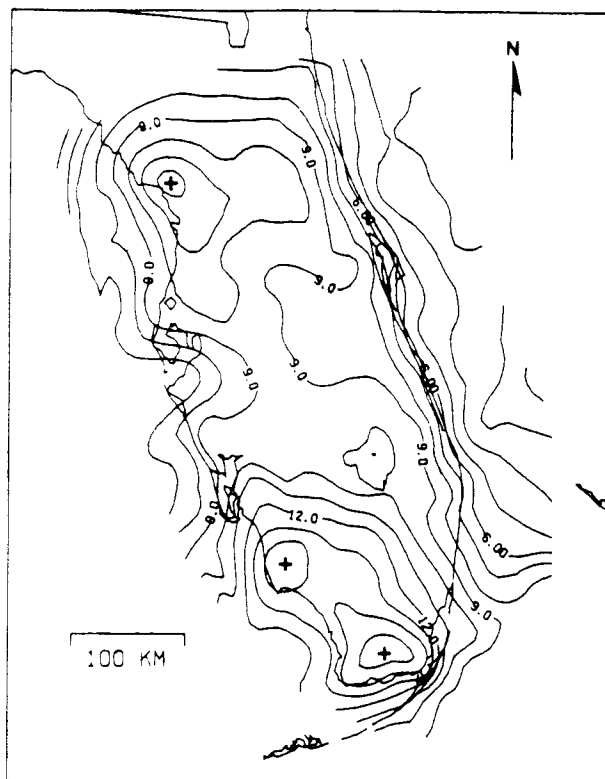


Fig. 4. Mean percent of hours that a MDR VIP return of 3.0 or greater was observed (from Michaels *et al.*, 1987).

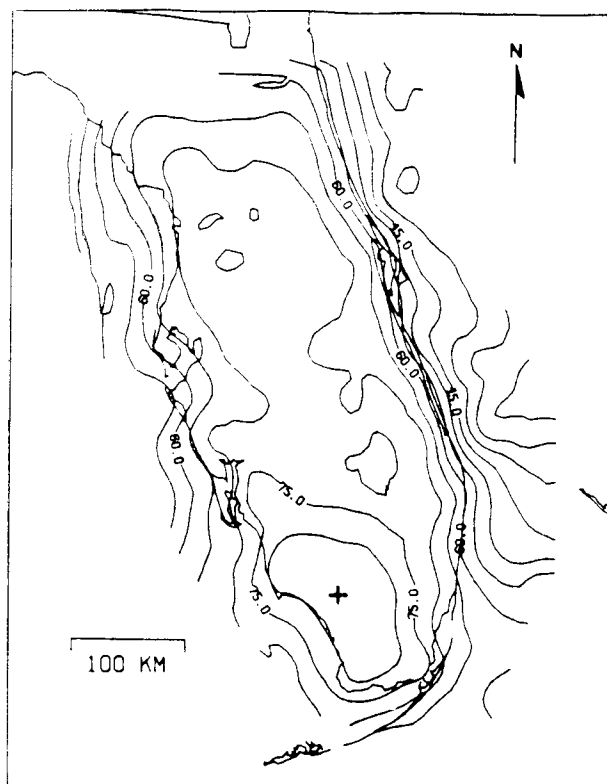


Fig. 5. Mean percent of summer (June-August) days in which a MDR return of 3.0 or greater was observed (from Michaels *et al.*, 1987).

Michaels *et al.* (1987) further decomposed the MDR data into empirical orthogonal functions (EOF) related to MDR returns of three or greater for each of the 150 grid cells used in the analysis. Figure 6a illustrates the first EOF pattern over Florida, along with the diurnal trend in its average value (Fig. 6b). Large positive EOF values are associated with above average thunderstorm activity. (The pattern is clearly related to Fig. 4, although the sum of all the EOFs are required to be able to reproduce Figure 4.) The first EOF explains 10.16% of the variance out of 53.96% which are explained by the 35 statistically significant EOFs. The diurnal variation of the first EOF (in Figure 6b) also closely corresponds to the 2-hour resolution variation in deep convective activity as seen from satellite (Figure 3).

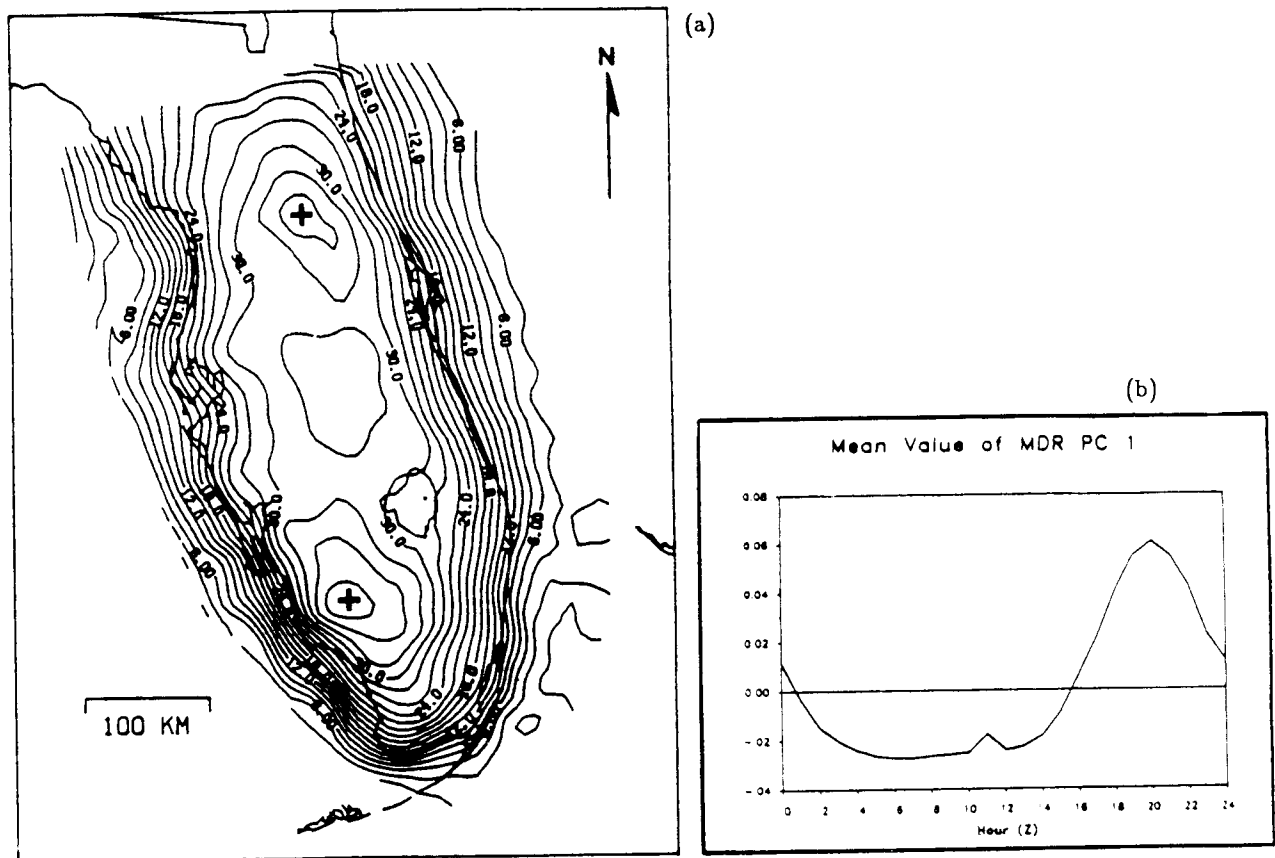


Fig. 6. (a) First EOF of MDR data ($\times 100$) and (b) mean hourly value (from Michaels *et al.*, 1987).

3. Modeling studies

In order to explain the observed preferential patterning of the deep cumulus convection over Florida, several mesoscale modeling studies are summarized below. The main focus of these model simulation are:

McQueen and Pielke, 1985:

To investigate the influences of synoptic geostrophic wind speed and direction, and vegetation and soil characteristics on the vertical motion and thermodynamic structure of the sea breeze

Lyons and Pielke, 1985; and
Lyons *et al.*, 1986:

To examine the spatial and temporal variations of available convective instability due to sea breeze convergence.

Song, 1986:

To examine the deep cumulus convective feedbacks to the sea breeze once thunderstorms occur, and to evaluate the importance of downdraft cooling on subsequent deep cumulonimbus development.

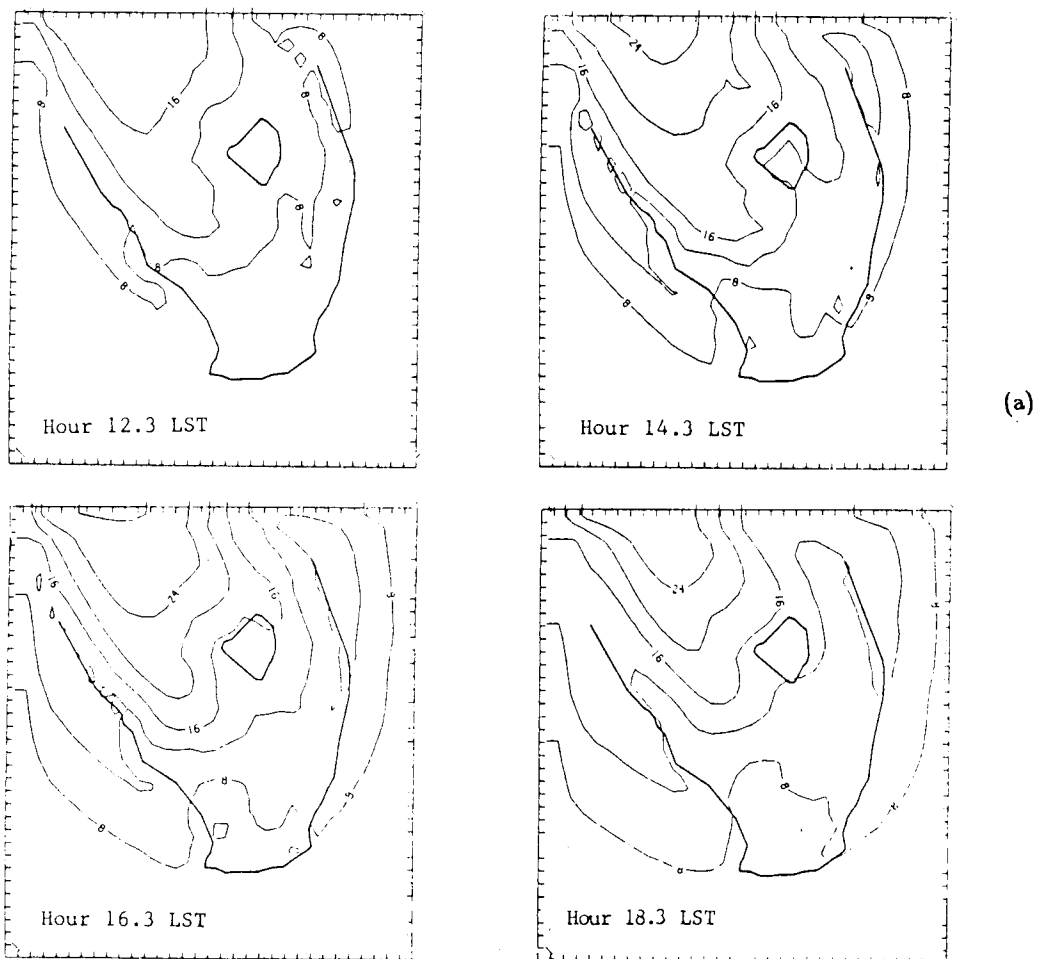


Fig. 7. (a) Simulated $\theta_{e,s} - \theta$ in $^{\circ}\text{K}$ at 500 for light, southeast synoptic geostrophic flow. (b) The horizontal wind field at 25 m for light southeast geostrophic synoptic flow (from McQueen and Pielke, 1985).

Figure 7 from McQueen and Pielke (1985) illustrates the mesoscale model predicted 25 m horizontal wind field and 500 m $\theta_{es} - \theta_e$ field at four times during the day for the light southeast geostrophic flow case mentioned in Section 2.2 and corresponding to the satellite composites in Figure 3. One of the conclusions from that study is that a combination of horizontal convergence in the boundary layer and a moister lower troposphere is conducive to deep cumulus convection.

The thermally forced mesoscale circulations over south Florida provide the focusing of the available buoyant convective energy. This available convective energy is enhanced in regions of higher evapotranspiration such as the Everglades, and reduced in regions west of Lake Okeechobee where sandy, dry soils exist.

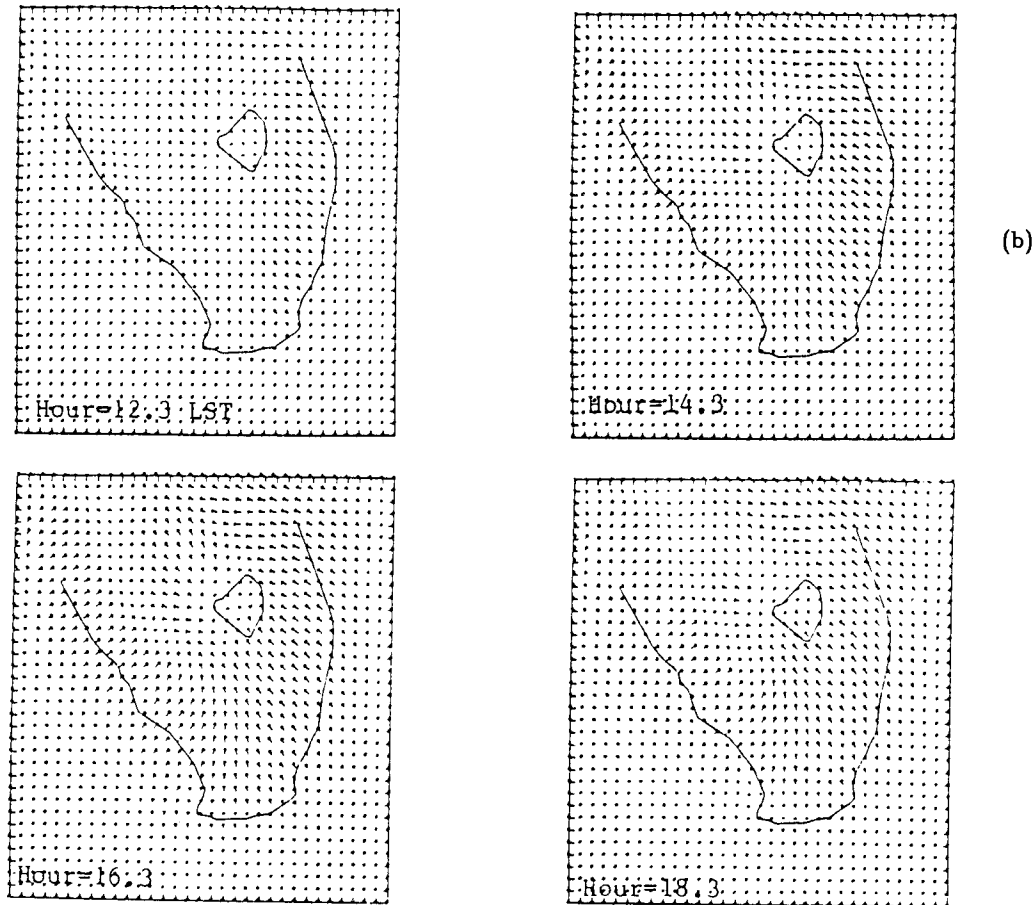


Figure 7 (continued)

Lyons and Pielke (1985) and Lyons *et al.* (1986) introduced a new index in order to more effectively evaluate the likelihood for deep convection on the mesoscale. Referred to as the “KLIW” index, it is an arbitrary linear combination of the K-index, the Lifted Index, and the model predicted vertical motion. Figure 8 presents an east-west time cross section of the KLIW index across central Florida, where the higher values were well-correlated with the observed patterning of thunderstorm evolution.

Using a cumulus parameterization within the mesoscale model, Song (1986) shows how secondary deep cumulus convection can develop as a result of the cooling of the boundary layer by

downrafts under and around cumulonimbus. A mesoscale pressure gradient and resultant low-level outflow develops between the cool region and the adjacent unmodified boundary layer air. Figure 9 illustrates an example of the perturbation of the horizontal divergence and potential temperature at 9 m from a dry sea breeze run as a result of the deep convection.

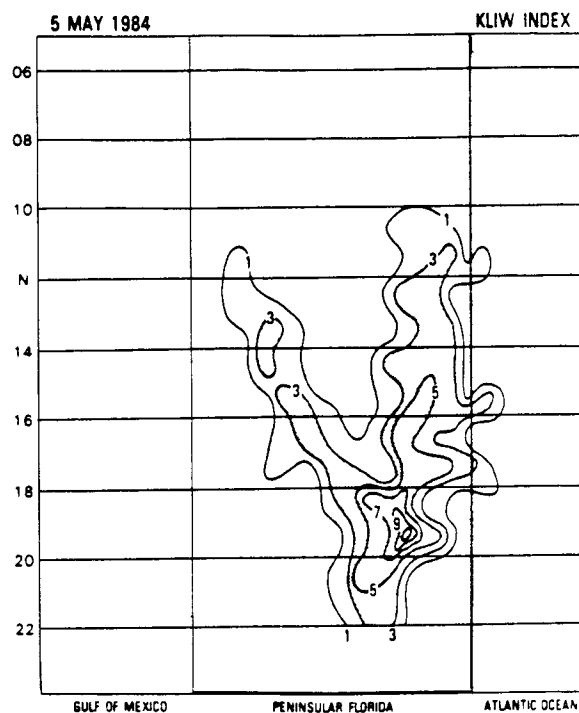


Fig. 8. XT time section of the KLIW Index, along an east-west section through KSC, derived from a mesoscale model simulation for 5 May 1983. Contours at 1, 3, 5, 7, 9 and 11 units (from Lyons *et al.*, 1985).

4. Conclusion

The satellite and radar analyses clearly illustrate preferential regions of thunderstorm occurrences over south Florida. The synoptic analysis suggests that a moister lower and middle troposphere is conducive to a greater percentage of coverage by these storms. The observed patterning of deep convection can be explained to a large extent by regions of enhanced mesoscale horizontal boundary layer convergence and resultant accumulation of lower tropospheric moisture. This convergence is enhanced in south Florida by the favorable curvature of the coastline (Pielke, 1984, pg. 458). A mesoscale model provides an effective tool to simulate the observed patterns as a function of synoptic wind and thermodynamic structure.

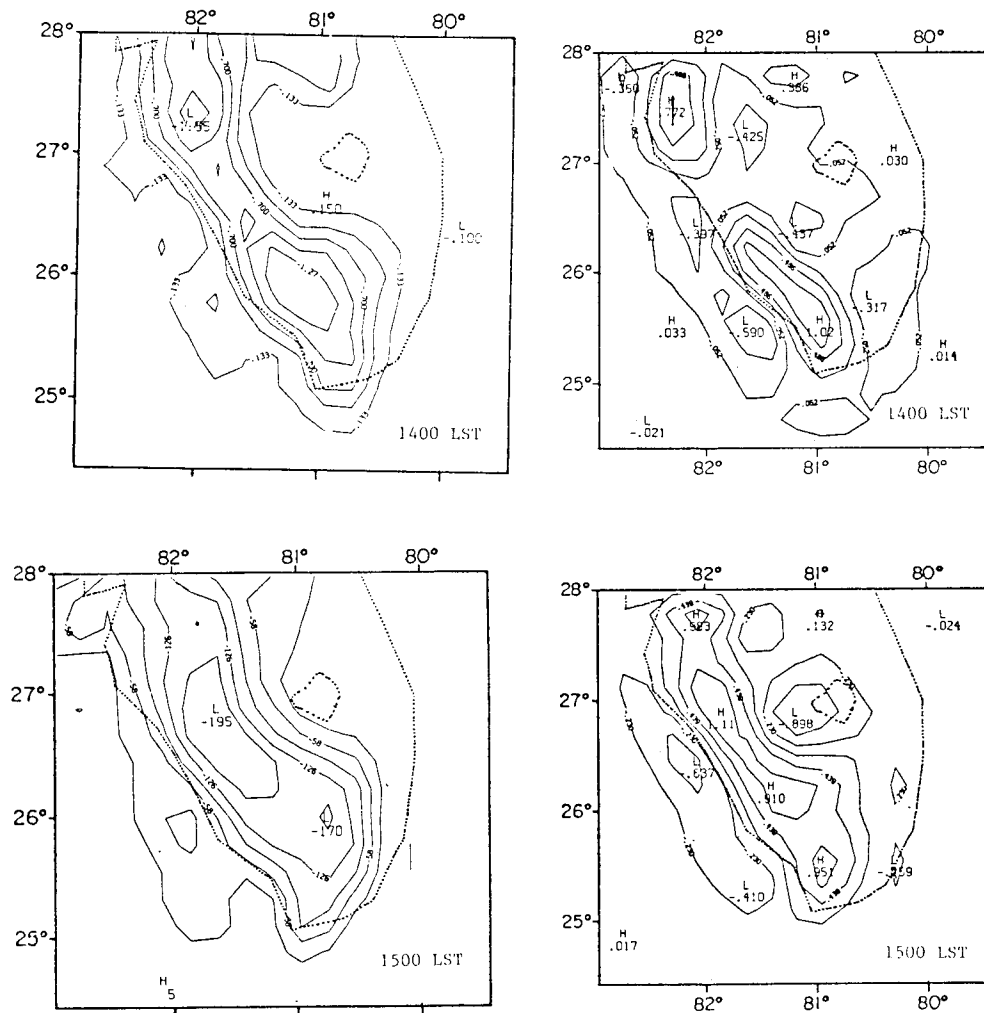


Fig. 9. Influence of deep cumulus convection on mesoscale horizontal divergence at 9 m and potential temperature at 9 m at 1400 LST and 1500 LST. Figures are obtained by subtracting a mesoscale model simulation without parameterized deep cumulus convection from an identical model simulation except with parameterized cumulonimbus convection (from Song, 1986).

In summary, the mesoscale influences the preexisting synoptic environment so as to provide preferential areas of thunderstorm activity. Using a combination of radar, satellite, synoptic observations, and mesoscale modeling tools, effective predictions of the percent coverage, and spatial and temporal distribution of thunderstorms in the sea breeze environment anywhere in the world appears possible.

Acknowledgements

The authors acknowledge the support of NASA contract NAG5-359, NSF Grant ATM-8616662 and ATM-8915265, and University of Kansas GRF grant 3202-XX-0038. Computer calculations were

performed on the NCAR CRAY and on the Colorado State University CYBER 205 computers. NCAR is supported by the NSF. The typing and editorial preparation of this paper were handled by Mrs. Dallas McDonald.

REFERENCES

- Betts, A. K., 1974. Thermodynamic classification of tropical convective soundings. *Mon. Wea. Rev.*, **102**, 760-764.
- Burpee, R. W., 1979. Peninsula-scale convergence in the south Florida sea breeze. *Mon. Wea. Rev.*, **107**, 852-860.
- Hsu, S., 1969. Mesoscale structure of the Texas coast sea breeze. Report. No. 16, Atmospheric Science Group, University of Texas, College of Engineering, Austin.
- Lyons, W. A. and R. A. Pielke, 1985. Forecasting sea breeze thunderstorms using a mesoscale numerical model. Final Report, R*SCAN Corporation, submitted to NASA, contract #NAS10-11142, August 1985.
- Lyons, W. A., J. A. Schuh, R. A. Pielke and M. Segal, 1986. Forecasting sea breeze thunderstorms at the Kennedy Space Center using the prognostic three-dimensional mesoscale model. *Eleventh Conference on Weather Forecasting and Analysis*, June 1986, Kansas City, Missouri.
- McQueen, J. T. and R. A. Pielke, 1985. A numerical and climatological investigation of deep convective cloud patterns in south Florida. Atmospheric Science Paper # 389, Department of Atmospheric Science, Colorado State University, Fort Collins, Colorado 177 pp.
- Michaels, P. J., R. A. Pielke, J. S. McQueen and D. E. Sappington, 1987. Composite climatology of Florida summer thunderstorms. *Mon. Wea. Rev.*, **115**, 2781-2791.
- Pielke, R. A., 1974. A three-dimensional numerical model of the sea breezes over south Florida. *Mon. Wea. Rev.*, **102**, 115-139.
- Pielke, R. A., 1984. Mesoscale meteorological modeling. Academic Press, New York, N. Y., 612 pp.
- Reap, R. M. and D. S. Foster, 1979. Automated 12-36 hour probability forecasts of thunderstorms and severe local storms. *J. Appl. Meteor.*, **18**, 1304-1315.
- Song, Jenn-Luen, 1986. Ph. D. Dissertation: A numerical investigation of Florida's sea breeze-cumulonimbus interactions. Department of Atmospheric Science, Colorado State University, 187 pp.